BioNanoSci. (2018) 8:299–303
DOI 10.1007/s12668-017-0447-6

PEG-Coated Superparamagnetic Dysprosium-Doped Fe_3O_4 Nanoparticles for Potential MRI Imaging

Timur Sh. Atabaev[1]

Published online: 30 August 2017

Abstract In recent years, superparamagnetic nanoparticles (NPs) have attracted considerable attention due to their high potential for biomedical applications. This study describes a facile preparation method of superparamagnetic polyethylene glycol (PEG)-coated dysprosium-doped Fe_3O_4 NPs for potential magnetic resonance imaging (MRI) applications. The structure, morphology, and magnetic properties of the dysprosium-doped Fe_3O_4 NPs were analyzed by X-ray diffraction (XRD), transmission electron microscopy (TEM), and quantum design vibrating sample magnetometer (QD-VSM), respectively. The MRI imaging ability of the dysprosium-doped Fe_3O_4 NPs was assessed using a 1.5-T small animal MRI scanner. In addition, pilot studies were performed to examine the toxicity of the PEG-coated dysprosium-doped Fe_3O_4 NPs. The obtained results suggested that prepared NPs could be used for potential T_2-weighted MRI imaging.

Keywords Dysprosium-doped Fe_3O_4 · Superparamagnetic nanoparticles · MRI imaging · Toxicity

1 Introduction

Superparamagnetic iron oxide NPs have been extensively used in various biomedical applications such as hyperthermia, image contrast enhancement, controlled drug delivery, cell tracking and sorting, etc. [1–5]. In particular, these superparamagnetic iron oxide NPs have a great potential for non-invasive in vivo MRI imaging [6, 7]. To date, several types of Fe_3O_4-based contrast agents (Feridex, Resovist) have been clinically approved for medical applications [8]. These contrast agents can generate strong MRI signal thanks to their ability to shorten the T_2 relaxation times in liver, spleen, and bone marrow. On the other hand, it is always of great scientific interest to develop the Fe_3O_4-based contrast agents with significantly improved magnetic properties for ultrasensitive MRI. From this point of view, various MFe_2O_4 (M = Mn, Co, Ni, Zn) NPs were developed as novel contrast agents [9, 10]. Thus, engineering of the MFe_2O_4 NPs becomes a hot trend in nanomedicine thanks to their unique magnetic properties and low toxicity. Recently, rare-earth (RE) ion-doped iron oxides were also prepared to investigate the coupling interactions between 4*f* orbitals of RE ions and 3*d* orbitals of transition metal ions. For example, Bloemen and co-workers investigated the effects of holmium Ho(III) doping into a Fe_3O_4 host [11]. According to their results, the resulting Ho-doped Fe_3O_4 NPs have lower saturation magnetization compared to the bare Fe_3O_4. At the same time, Huan and co-workers reported that small amount of dysprosium Dy(III) doping can enhance the magnetic properties of Fe_3O_4 NPs [12]. It is known that T_2 relaxation of water protons is proportional to the square of a total magnetic moment of NPs [13]. Thus, it is expected that Fe_3O_4 NPs doped with a small amount of Dy(III) ions may offer stronger MRI T_2 signal than that of bare Fe_3O_4 NPs. To the best of our knowledge, the potential of Dy(III)-doped Fe_3O_4 contrast agents for MRI imaging have not been investigated yet. Therefore, in this study we investigated the capability of PEG-coated Dy(III)-doped Fe_3O_4 NPs for potential T_2-weighted MRI imaging. In addition, pilot studies were performed to examine the toxicity of prepared PEG-coated Dy(III)-doped Fe_3O_4 NPs.

✉ Timur Sh. Atabaev
timuratabaev@yahoo.com; timur.atabaev@nu.edu.kz

[1] Department of Chemistry, School of Science and Technology, Nazarbayev University, Astana, Kazakhstan 010000

2 Experimental

2.1 Synthesis and Characterization

Ferric chloride hexahydrate ($FeCl_3 \cdot 6H_2O$, ≥ 99%), ferrous chloride tetrahydrate ($FeCl_2 \cdot 4H_2O$, 99.99%), dysprosium chloride hexahydrate ($DyCl_3 \cdot 6H_2O$, 99.9%), polyethylene glycol (PEG, average M_n 4000), and ammonium hydroxide (NH_4OH, 28.0–30.0%) were purchased from Sigma-Aldrich and used as received. The PEG-coated Dy(III)-doped Fe_3O_4 NPs were prepared using a reported protocol with slight modification (Dy(III) addition) [14]. The doping concentration of Dy(III) ions was kept at optimal 1 mol% [12]. The obtained NPs were then dialyzed in deionized water for 24 h to eliminate the unreacted products.

The structure of the prepared powders was examined by X-ray diffraction (XRD, Bruker D8 Discover) using Cu-Kα radiation (λ = 0.15405 nm) at a 2θ scan range 20–60° 2θ. The morphology of the nanoparticles was characterized by transmission electron microscopy (TEM, JEOL JEM-2100). Hydrodynamic sizes and zeta potentials of the obtained nanoprobes were measured using a Nano ZS Zetasizer. Fourier transform infrared spectroscopy (FTIR, Bruker Tensor 27) was utilized to examine the structural properties of prepared sample. Inductively coupled plasma optical emission spectrometry (ICP-OES, Avio 500, PerkinElmer) was utilized for Dy(III) quantification. The magnetization measurements were performed using a quantum design vibrating sample magnetometer (QD-VSM, PPMS 6000). The T_2-weighted images were obtained using a 1.5-T small animal MRI scanner (Siemens). The measurement parameters used were as follows: TR/TE = 2009 ms/9 ms, field of view (FOV) = 160 mm × 160 mm, slice thickness = 5 mm, matrix = 256 × 256, and number of excitations (NEX) = 1. All measurements were performed at a room temperature of 22 ± 1 °C.

2.2 Cell Culture and Cytotoxicity Assay

A murine fibroblast cell line (L-929 cells from subcutaneous connective tissue) was obtained from the American Type Culture Collection (ATCC CCL-1™, Rockville, MD). The cells were routinely maintained in Dulbecco's modified Eagle's medium (Sigma-Aldrich), supplemented with 10% fetal bovine serum (Sigma-Aldrich) and 1% antibiotic antimycotic solution (including 10,000 units penicillin, 10 mg streptomycin, and 25 mg amphotericin B per ml, Sigma-Aldrich) at 37 °C in 95% humidity and 5% CO_2. The number of viable cells was indirectly quantified using highly water-soluble tetrazolium salt [WST-8,2-(2-methoxy-4-nitrophenyl)-3-(4-nitrophenyl)-5-(2,4-disulfophenyl)-2*H*-tetrazolium, monosodium salt] (Dojindo Lab., Kumamoto, Japan), reduced to a water-soluble formazan dye by mitochondrial dehydrogenases. The cell viability was found to be directly proportional to the metabolic reaction products obtained in WST-8. Briefly, the WST-8 assay was conducted as follows. L-929 cells were treated with increasing concentration (0–512 μg/ml) of nanoprobes and then incubated with WST-8 for the 24 h at 37 °C in the dark. Parallel sets of wells containing freshly cultured nontreated cells were regarded as negative controls. The absorbance was determined to be 450 nm using an ELISA reader (SpectraMax® 340, Molecular Device Co., Sunnyvale, CA). The relative cell viability was determined as the percentage ratio of the optical densities in the medium (containing the nanoprobes at each concentration) to that of the fresh control medium.

2.3 Statistical Analysis

All variables were tested in three independent cultures for cytotoxicity assay, which was repeated twice (n = 6). Quantitative data are expressed as the mean ± standard deviation (SD). A value of $p < 0.05$ was considered statistically significant.

3 Results and Discussion

XRD analysis was utilized to examine the structural properties of as-prepared Dy-doped Fe_3O_4 NPs. Figure 1 shows that all peaks of Dy-doped Fe_3O_4 NPs can be indexed to the face-centered cubic magnetite structure (JCPDS no. 19-0629) [4, 15]. No additional peaks were detected mainly due to low Dy(III) doping amount. Thus, obtained results suggest that it is possible to prepare Dy-doped Fe_3O_4 NPs without disturbing the single-phase magnetite structure. ICP-OES analysis was further employed to reveal the actual Dy(III) dopant amount in

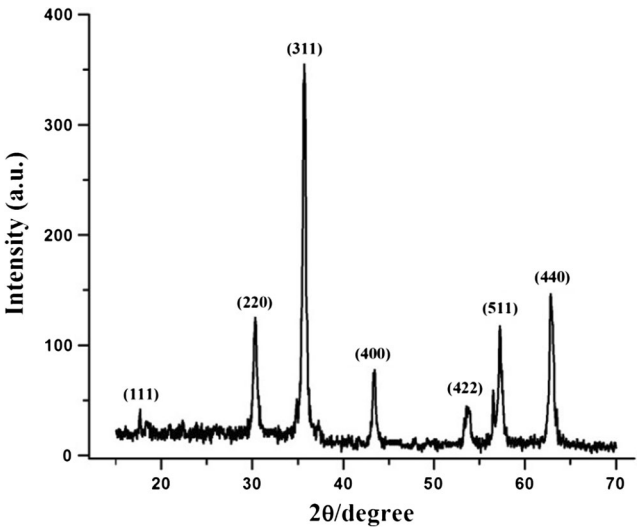

Fig. 1 XRD pattern of as-prepared Dy-doped Fe_3O_4 NPs

Fe_3O_4. ICP-OES measurements showed that the actual doping amount of Dy(III) in Fe_3O_4 is 0.53 ± 0.04 mol%. Thus, it can be concluded that the real doping of Dy(III) in Fe_3O_4 is approximately half of the inserted during the synthesis. This is most likely due to the scenario that Dy-doping leads to increased distortions in the magnetite structure, which is kinetically unfavored.

Figure 2 shows the morphology and size distribution of the PEG-coated Dy(III)-doped Fe_3O_4 NPs. The average sizes of quasi-spherical PEG-coated Dy(III)-doped Fe_3O_4 NPs measured with the help of TEM were in the range of 9–13 nm (based on 100 nanoparticle counts). However, the measured average hydrodynamic sizes of the PEG-coated Dy(III)-doped Fe_3O_4 NPs were in the range of 12–18 nm. The existence of a thin PEG-coating layer and a hydration coverage on the surface of Dy-doped Fe_3O_4 NPs can explain the observed size difference [16]. FTIR analysis was further performed to verify the successful PEG coating on the surface of Dy-doped Fe_3O_4 NPs. Figure 3 shows the spectrum of PEG-coated Dy(III)-doped Fe_3O_4 NPs measured in the range of 400–4000 cm^{-1}. Two absorption bands around 565 and 421 cm^{-1} are characteristic signals (Fe-O bonds) of nanosized magnetite [17]. Another two absorption bands at 1633 and 3448 cm^{-1} were assigned to angular deformation of water molecules and deformation vibrations of hydroxyl groups, respectively [16]. The most prominent peak at ~ 1100 cm^{-1} was assigned to the C-O-C vibration of PEG chain [16]. Thus, FTIR analysis highlights the presence of water molecules and PEG on the surface of Dy-doped Fe_3O_4 NPs. The measured zeta potential of PEG-coated Dy(III)-doped Fe_3O_4 NPs at the physiological pH of 7.4 was − 17.1 mV. Thus, the PEG coating helps to maintain the colloidal stability of Dy-doped Fe_3O_4 NPs and prolong their in vivo circulation time [18].

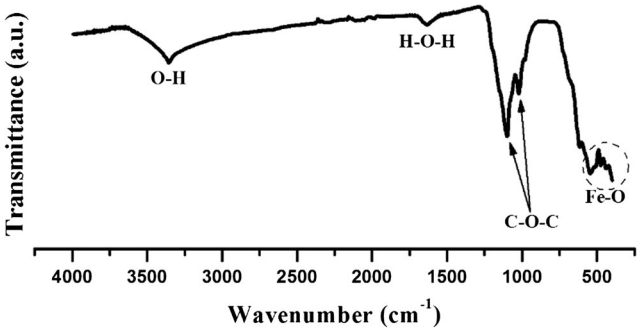

Fig. 3 FTIR analysis of PEG-coated Dy(III)-doped Fe_3O_4 NPs

QD-VSM was employed to examine the superparamagnetic properties of prepared samples. For comparison, undoped PEG-coated Fe_3O_4 NPs were also synthesized using the same synthesis protocol. Figure 4 shows the magnetization curves M(H) of PEG-coated Dy-doped Fe_3O_4 NPs and undoped PEG-coated Fe_3O_4 NPs measured at 300 K. The coercivity for both samples was negligible, indicating the typical superparamagnetic behavior. Saturation magnetization for undoped PEG-coated Fe_3O_4 NPs and PEG-coated Dy-doped Fe_3O_4 NPs were equal to 35.2 and 39.1 emu g-1, respectively. Thus, it can be concluded that Dy(III) addition can enhance the magnetization of the Fe_3O_4 NPs at low doping concentrations [12]. PEG-coated Dy-doped Fe_3O_4 NPs with enhanced magnetization can be potentially utilized for high-resolution T_2-weighted MRI imaging.

The small animal 1.5-T MRI scanner was further used to assess the MRI imaging ability of the PEG-coated Dy-doped Fe_3O_4 NPs. Figure 5 shows that PEG-coated Dy-doped Fe_3O_4 NPs are able to affect the T_2-weighted signal in a concentration-dependent manner. The relaxivity rate (R_2) of PEG-coated Dy-doped Fe_3O_4 NPs was calculated using a

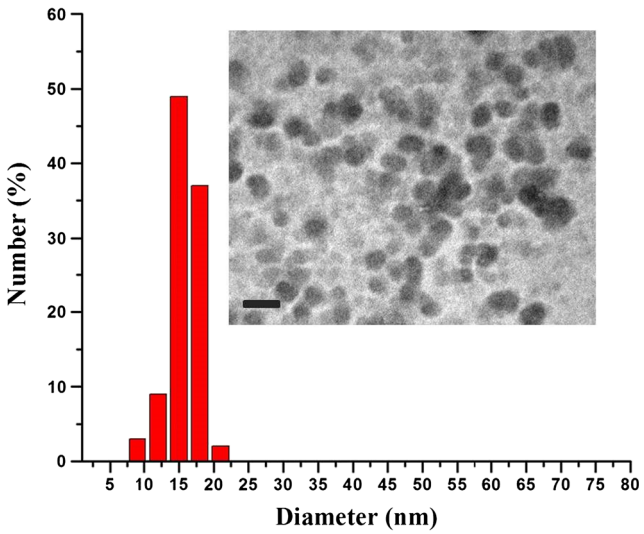

Fig. 2 Hydrodynamic sizes of PEG-coated Dy(III)-doped Fe_3O_4 NPs. Inset is TEM image of PEG-coated Dy(III)-doped Fe_3O_4 NPs (scale bar = 20 nm)

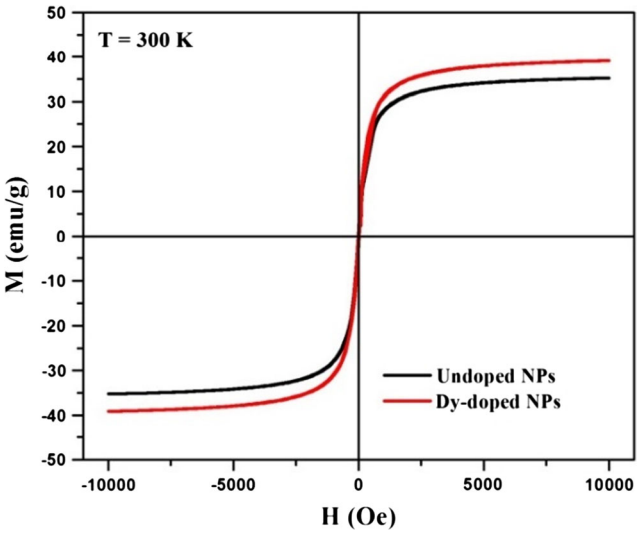

Fig. 4 Magnetization curves of PEG-coated undoped and Dy-doped Fe_3O_4 NPs

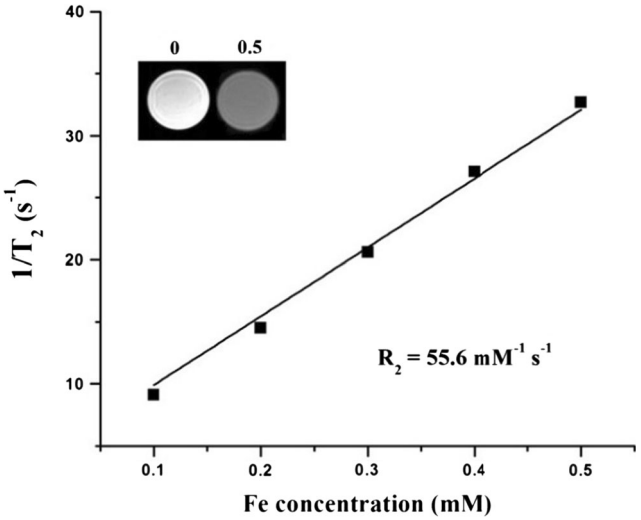

Fig. 5 Room temperature R_2 relaxation rate ($1/T_2$) vs. iron concentration (mM). Inset is T_2-weighted MRI phantom images of aqueous solutions without and with PEG-coated Dy-doped Fe_3O_4 NPs

slope of the linear plot of the relaxation rate ($R_2 = 1/T_2$) vs. Fe concentration (mM). Figure 5 clearly shows that the transverse relaxation of water protons increases with the iron concentration increasing. The linear plot of transverse relaxation yields $R_2 = 55.6 \pm 2.1$, which is much higher than that of commercial MRI contrast agent Feridex ($R_2 = 41 \pm 2$) [19]. The T_2-weighted MRI phantom test of aqueous solutions without and with PEG-coated Dy-doped Fe_3O_4 NPs (0.5 mM) was also included for comparison. Figure 5 (inset) shows that the aqueous solutions with PEG-coated Dy-doped Fe_3O_4 NPs become darker under magnetic field. Thus, the prepared PEG-coated Dy-doped Fe_3O_4 NPs with enhanced T_2 relaxation rate can be potentially applied for contrast enhancement during the MRI imaging.

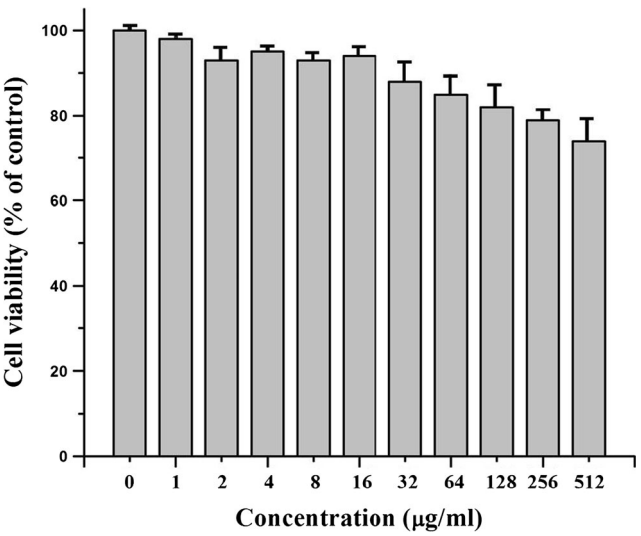

Fig. 6 Cytotoxicity profiles of the PEG-coated Dy-doped Fe_3O_4 NPs in L-929 cells

The toxicity tests were performed to evaluate the feasibility of using PEG-coated Dy-doped Fe_3O_4 NPs as a potential MRI contrast agent. Figure 6 shows the cytotoxicity profiles of the PEG-coated Dy-doped Fe_3O_4 NPs in L-929 fibroblastic cells using a WST-8 assay. According to the cytotoxicity results, nearly 94% of the L-929 cells can be survived at low concentrations (up to 16 μg/ml) during the 24 h of the incubation period. On the other hand, the toxicity of the PEG-coated Dy-doped Fe_3O_4 NPs dramatically increased at higher (≥ 32 μg/ml) concentrations probably due to so-called "Trojan horse" mechanism [20]. Thus, it can be concluded that PEG-coated Dy-doped Fe_3O_4 NPs can be safely used at concentrations less than 16 μg/ml (considering the in vitro cytotoxicity only). But, the toxicity of the PEG-coated Dy-doped Fe_3O_4 NPs must be also tested by other viability end-point measurements.

4 Conclusions

PEG-coated Dy-doped Fe_3O_4 NPs were successfully prepared for potential T_2-weighted MRI imaging. We showed that magnetization of Fe_3O_4 NPs can be enhanced by moderate Dy-doping. As a result, PEG-coated Dy-doped Fe_3O_4 NPs demonstrated enhanced relaxivity rate compared to the commercially available MRI contrast agent Feridex. In addition, the in vitro cytotoxicity results suggested that PEG-coated Dy-doped Fe_3O_4 NPs can be safely used at concentrations less than 16 μg/ml. Overall, the prepared PEG-coated Dy-doped Fe_3O_4 NPs with improved R_2 relaxivity rate have high potential for sensitive T_2-weighted MRI imaging.

Acknowledgments We would like to thank Ms. Gulnoza Urmanova (Department of Biotechnology, NUUz) for cytotoxicity measurements. We would also like to thank the funding grant provided by NU to conduct the preliminary research.

References

1. Atabaev, T. S. (2016). Multimodal inorganic nanoparticles for biomedical applications. In A. M. Grumezescu (Ed.), *Nanobiomaterials in medical imaging: applications of nanobiomaterials* (pp. 253–278). Amsterdam: Elsevier Inc..
2. Lv, Y., Yang, Y., Fang, J., et al. (2015). Size dependent magnetic hyperthermia of octohedral Fe_3O_4 nanoparticles. *RSC Advances, 5*, 76764–76771.
3. Mustapic, M., Hossain, M. S. A., Horvat, J., et al. (2016). Controlled delivery of drug adsorbed onto porous Fe_3O_4 structures by application of AC/DC magnetic fields. *Microporous and Mesoporous Materials, 226*, 243–250.
4. Atabaev, T. S., Kim, H. K., & Hwang, Y. H. (2013). Fabrication of bifunctional core-shell Fe_3O_4 particles coated with ultrathin phosphor layer. *Nanoscale Research Letters, 8*, 357.
5. Lu, W., Ling, M., Jia, M., Huang, P., Li, C., & Yan, B. (2014). Facile synthesis and characterization of polyethylenimine-coated Fe_3O_4 superparamagnetic nanoparticles for cancer cell separation. *Molecular Medicine Reports, 9*, 1080–1084.

6. German, S. V., Navolokin, N. A., Kuznetsova, N. R., et al. (2015). Liposomes loaded with hydrophilic magnetite nanoparticles: preparation and application as contrast agents for magnetic resonance imaging. *Colloids and Surfaces, B: Biointerfaces, 135*, 109–115.
7. Ozdemir, A., Ekiz, M. S., Dilli, A., Guler, M. O., & Tekinay, A. B. (2016). Amphiphilic peptide coated superparamagnetic iron oxide nanoparticles for in vivo MR tumor imaging. *RSC Advances, 6*, 45135–45146.
8. Wang, Y. X. J. (2015). Current status of superparamagnetic iron oxide contrast agents for liver magnetic resonance imaging. *World Journal of Gastroenterology, 21*, 13400–13402.
9. Wang, Z., Liu, J., Li, T., Liu, J., & Wang, B. (2014). Controlled synthesis of of $MnFe_2O_4$ nanoparticles and Gd complex-based nanocomposites as tunable and enhanced T_1/T_2-weighted MRI contrast agents. *Journal of Materials Chemistry B, 2*, 4748–4753.
10. Barcena, C., Sra, A. K., Chaubey, G. S., Khemtong, C., Liu, J. P., & Gao, J. (2008). Zinc ferrite nanoparticles as MRI contrast agents. *Chemical Communications, 2008*, 2224–2226.
11. Bloemen, M., Vandendriessche, S., Goovaerts, V., et al. (2014). Synthesis and characterization of holmium doped iron oxide nanoparticles. *Materials, 7*, 1155–1164.
12. Huan, W., Ji, G., Cheng, C., An, J., Yang, Y., & Liu, X. (2015). Preparation, characterization of high-luminescent and magnetic Eu3+, Dy3+ doped superparamagnetic nano-Fe3O4. *Journal of Nanoscience and Nanotechnology, 15*, 1780–1788.
13. Xu, W., Kattel, K., Park, J. Y., Chang, Y., Kim, T. J., & Lee, G. H. (2012). Paramagnetic nanoparticle T_1 and T_2 MRI contrast agents. *Physical Chemistry Chemical Physics, 14*, 12687–12700.
14. Thapa, B., Diaz-Diestra, D., Beltran-Huarac, J., Weiner, B. R., & Morell, G. (2017). Enhanced MRI T_2 relaxivity in contrast-probed anchor-free PEGylated iron oxide nanoparticles. *Nanoscale Research Letters, 12*, 312.
15. Atabaev, T. S., Lee, J. H., Lee, J. J., et al. (2013). Mesoporous silica with fibrous morphology: a multifunctional core-shell platform for biomedical applications. *Nanotechnology, 24*, 345603.
16. Atabaev, T. S., Shin, Y. C., Song, S. J., Han, D. W., & Hong, N. H. (2017). Toxicity and T_2-weighted magnetic resonance imaging potentials of holmium oxide nanoparticles. *Nanomaterials, 7*, 216.
17. Karimzadeh, I., Aghazadeh, M., Doroudi, T., et al. (2017). Superparamagnetic iron oxide (Fe3O4) nanoparticles coated with PEG/PEI for biomedical applications: a facile and scalable preparation route based on cathodic electrochemical deposition method. *Adv Phys Chem, 2017*, 9437487.
18. Atabaev, T. S., Lee, J. H., Han, D. W., Kim, H. K., & Hwang, Y. H. (2014). Ultrafine PEG-capped gadolinia nanoparticles: cytotoxicity and potential biomedical applications for MRI and luminescent imaging. *RSC Advances, 4*, 34343–34349.
19. Rohrer, M., Bauer, H., Mintorovitch, J., Requardt, M., & Weinmann, H. J. (2005). Comparison of magnetic properties of MRI contrast media solutions at different magnetic field strengths. *Investigative Radiology, 40*, 715–724.
20. Atabaev, T. S., Lee, J. H., Shin, Y. C., et al. (2017). Eu, Gd-codoped yttria nanoprobes for optical and T_1-weighted magnetic resonance imaging. *Nanomaterials, 7*, 35.